



## Strong magnetic anisotropy of epitaxial PrVO<sub>3</sub> thin films on SrTiO<sub>3</sub> substrates with different orientations

D Kumar, P Boullay, A Fouchet, A David, A Pautrat, Wilfrid Prellier, Chang Uk Jung

### ► To cite this version:

D Kumar, P Boullay, A Fouchet, A David, A Pautrat, et al.. Strong magnetic anisotropy of epitaxial PrVO<sub>3</sub> thin films on SrTiO<sub>3</sub> substrates with different orientations. ACS Applied Materials & Interfaces, 2020, 12 (31), pp.35606-35613. 10.1021/acsami.0c07794 . hal-03019085

**HAL Id: hal-03019085**

**<https://hal.science/hal-03019085>**

Submitted on 23 Nov 2020

**HAL** is a multi-disciplinary open access archive for the deposit and dissemination of scientific research documents, whether they are published or not. The documents may come from teaching and research institutions in France or abroad, or from public or private research centers.

L'archive ouverte pluridisciplinaire **HAL**, est destinée au dépôt et à la diffusion de documents scientifiques de niveau recherche, publiés ou non, émanant des établissements d'enseignement et de recherche français ou étrangers, des laboratoires publics ou privés.

# Strong magnetic anisotropy of epitaxial $\text{PrVO}_3$ thin films on $\text{SrTiO}_3$ substrates with different orientations

D. Kumar,<sup>1\*</sup> P. Boullay,<sup>1</sup> A. Fouchet,<sup>1</sup> A. David,<sup>1</sup> A. Pautrat,<sup>1</sup> W. Prellier<sup>1\*</sup>

<sup>1</sup>*Laboratoire CRISMAT, CNRS UMR 6508,*

*ENSICAEN, Normandie Université,*

*6 Bd Maréchal Juin, F-14050 Caen Cedex 4, France*

## Abstract

We have probed the structural and magnetic properties of  $\text{PrVO}_3$  (PVO) thin films grown on the (001)-, (110)- and (111)-oriented  $\text{SrTiO}_3$  (STO) substrates. By changing the substrate orientation, (1) the out-of-plane orientation of film can be tuned to  $[110]$ ,  $[100]$  /  $[010]$ , and  $[011]$  /  $[311]$ , (2) the number of crystal variants in the film can be varied, for ex. we observe single domain film on (110)-oriented STO, whereas two domains in the film grown on the (111)-oriented STO substrate. The lattice strain induced by using different oriented substrates has direct influence on the magnetic properties of PVO films. The magnetic moment of PVO films radically enhances from  $0.4 \mu_B$  /f.u. for STO (001) to  $2.3 \mu_B$  /f.u. for STO (111). While, films on (001)-oriented STO substrate display out-of-plane anisotropy, an in-plane anisotropy is observed for films grown on the (110)- and (111)-oriented STO substrates. In addition, a strong uniaxial magnetic anisotropy is also extracted for a partially relaxed film on the (110)- oriented STO substrate. Such findings can help oxide community in the better understanding of magnetic anisotropy in vanadate thin films, a subject that still lacks scientific investigations.

PACS numbers: 81.15.Fg, 73.50.Lw, 68.37.Lp, 68.49.Jk

---

\*deepak.kumar@ensicaen.fr, wilfrid.prellier@ensicaen.fr

## I. INTRODUCTION

The  $RVO_3$ , where  $R$  is a trivalent rare earth element ( $R = \text{La, Ce, Pr, ..., Lu}$ ), have been intensively studied due to their wide range of physical properties [1–5]. In these compounds, the interaction between spin, orbit and lattice degrees of freedom remains the center of all intriguing physical phenomena, where one alters the ideal lattice of a compound in order to modify and even achieve new functionalities. These systems order with one of two different types of magnetic structures. For the compounds with larger rare earth radii ( $R = \text{La–Dy}$ ) the magnetic structure is of C-type (where, spins order antiferromagnetically along  $ab$  plane and ferromagnetically along the  $c$ -axis), whereas compounds with smaller rare earth radii ( $R = \text{Ho–Lu}$ ) have a G-type magnetic structure (spins order antiferromagnetically in all the direction) [6].

Bulk  $\text{PrVO}_3$  (PVO), at room temperature, adopts an orthorhombic  $Pbnm$  crystal structure with the lattice parameters:  $a_o = 5.487 \text{ \AA}$ ,  $b_o = 5.564 \text{ \AA}$ , and  $c_o = 7.778 \text{ \AA}$  ( $o$  stands for orthorhombic) [7]. Bulk PVO is a canted antiferromagnet [8], but it has tendency to become a hard ferromagnet when grown under epitaxial strain in the form of a thin film [9]. The impact of epitaxial strain imposed by the underlying substrate also plays a crucial role in governing the magnetism of the PVO films. Namely, when PVO films are grown on the  $\text{LaAlO}_3$  (LAO) substrate, under a large compressive strain (2.9 %), the reduction in in-plane bond length between neighboring V atoms leads to promote the super-exchange interactions, and thus exhibit large Néel temperature ( $T_N$ ). While, films grown on the  $\text{SrTiO}_3$  (STO) substrate under a moderate tensile strain ( $\sim 0.1 \%$ ) show reduced  $T_N$ , in agreement with our theoretical calculations [2]. Recent advances in the technological devices allow one to realize materials in the realm of atomic resolution, and separate the effect of epitaxial strain from microstructure and defects. Through X-ray Photoelectron Spectroscopy (XPS), the formation of an over-oxidized dead-layer (4–5 nm) on the surface of PVO film was earlier revealed, consisting of isolated Pr atom. Furthermore, this dead-layer has a large paramagnetic contribution, whose impact gradually diminishes with the increase of film thickness [10]. The over-oxidation of the film surface is quite common in vanadium oxide thin films, which tends to oxidize during growth process [11, 12]. One therefore needs to be very careful during thin film-fabrication and require additional precautions to avoid the surface oxidation, such as using of high vacuum during growth and reduction of film surface by using a capping layer.

The preferential direction of magnetization in thin films is mainly determined by the mag-

netic anisotropy, which includes shape anisotropy, magnetoelastic anisotropy and magnetocrystalline anisotropy. There have been numerous studies in the past to explore magnetic anisotropy in other competitive complex systems such as manganites [13–15], and ruthenates [16, 17], and due to Tunneling Magnetoresistance properties of the former, they are being used as Magnetic Tunneling Junction devices. However, little is known of the magnetic anisotropy in vanadium oxide thin films, especially PVO, and thus has yet to be understood.

In this paper, we were motivated to study the substrate surface orientation-induced magnetic anisotropy in PVO thin films, which were grown on (001)-, (110)- and (111)-oriented STO substrates. By changing the substrate-surface orientation, the out-of-plane orientation of PVO films can be effectively controlled. For the film grown on (111)-oriented STO substrate, we observe a striking enhancement in magnetization compared to its bulk counterpart, and, to our knowledge, is first time ever recorded. Furthermore, a strong in-plane uniaxial anisotropy is seen for film grown on the (110)-oriented STO substrate.

## II. EXPERIMENTAL

The  $\text{PrVO}_3$  (PVO) thin films were synthesized by using Pulsed Laser Deposition (PLD) on the (001)-, (110)- and (111)-oriented  $\text{SrTiO}_3$  (STO) substrates supplied by CrysTec. A KrF excimer laser (wavelength  $\lambda = 248$  nm) with repetition rate of 2 Hz and laser fluence of 2 J/cm<sup>2</sup> was focused on a  $\text{PrVO}_4$  ceramic target, with substrate-to-target distance of 5 cm. The growth temperature and pressure during deposition were maintained at 650 °C, and  $10^{-6}$  mbar, respectively. X-ray diffraction and reciprocal lattice mapping were performed on a Bruker D8 Discover diffractometer (Cu  $K\alpha 1$  radiation,  $\lambda = 1.5406$  Å) to study the crystallinity and strain states of the epitaxial layers. The film thickness was estimated by fitting the thickness fringes around Bragg peak of substrate to the Laue equation (*Intensity of oscillations*,  $I = \frac{\sin^2(NQC/2)}{\sin^2(QC/2)}$ ; where  $N$  is the number of unit cells,  $Q$  is the reciprocal lattice vector, and  $C$  denotes the out-of-plane lattice parameter). The microstructure of films on (110)- and (111)-oriented STO was revealed through Transmission Electron Microscopy (TEM) (**Description of TEM instrument**). The field- and temperature-dependent magnetization measurements were performed in a Quantum Design Magnetic Property Measurement System (MPMS) XL, as well as the Vibrating Sample Magnetometer (MPMS 3).

### III. STRUCTURE

The X-ray diffraction results of 35 nm thick PVO films grown on (001)-, (110)- and (111)-oriented STO substrates are detailed in Fig. 1. The Laue oscillations in the  $\theta$ - $2\theta$  High Resolution X-ray diffraction (HRXRD) patterns of PVO films on (001)- and (110)-oriented STO are indicative of a well-defined film-substrate interfaces, whereas, hardly an oscillation is observed for the film grown on (111)-oriented STO substrate. For STO (111) substrate, the polar catastrophe and intermix termination could invoke major reconstructions, and this could lead to produce rough interfaces [18]. The pseudocube interplanar spacings derived from the film peak positions in Figs. 1(a), 1(b), 1(c), are:  $d_{001} = 3.94 \text{ \AA}$ ,  $d_{110} = 3.98/\sqrt{2} = 2.814 \text{ \AA}$  and  $d_{111} = 3.954/\sqrt{3} = 2.283 \text{ \AA}$ , for PVO films on (001)-, (110)- and (111)-oriented STO substrates, respectively.

Reciprocal Space Maps (RSM) of PVO films on STO substrates were collected for the skew symmetrical reflections of the substrates (Fig. 2). The inspection of these maps reveals that the films have grown coherently on the STO substrates, with the same in-plane lattice

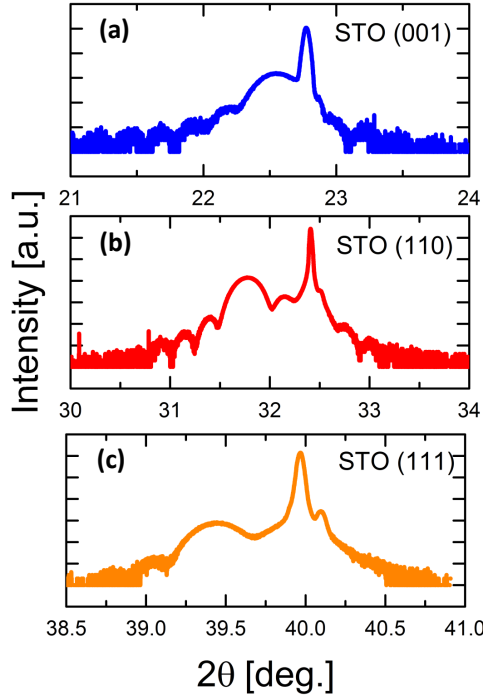


Figure 1: (Color online) HRXRD  $\theta - 2\theta$  scans of  $\text{PrVO}_3$  (PVO) thin films on (a) (001)-, (b) (110)- and (c) (111)-oriented  $\text{SrTiO}_3$  (STO) substrates, in the vicinity of  $(001)_c$ ,  $(110)_c$  and  $(111)_c$  Bragg's peak of STO, respectively. The subscript  $c$  refers to cubic.

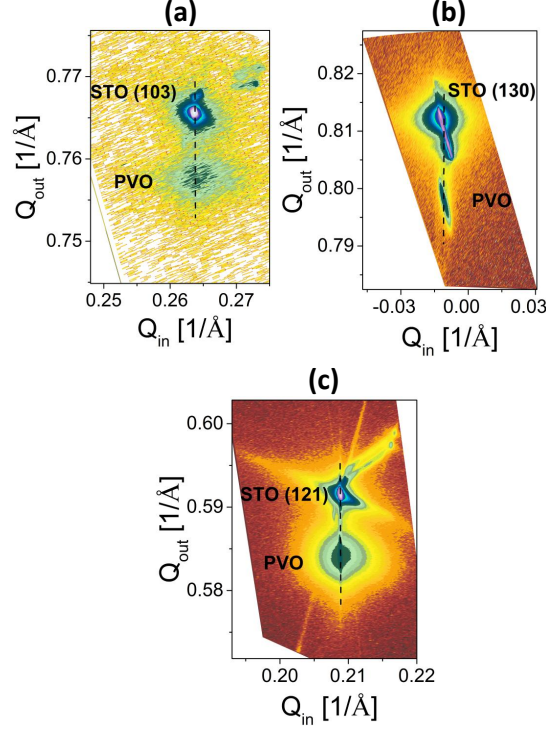


Figure 2: (Color online) X-ray diffraction reciprocal space maps around (d) STO (103), (e) STO (130) and (f) STO (121) of (001)-, (110)- and (111)-oriented STO substrates, respectively. The dashed lines are only guide to the eyes and represent strained nature of films with the substrates.

parameters, as the position of film peak along the horizontal  $Q_{in}$  axis matches with that of the substrate peak for all three orientations of the substrate. Combining the HRXRD  $\theta - 2\theta$  and RSM measurements, we have calculated the pseudocube unit-cell volume of PVO:  $V_{pc} = 3.905^2 \times 3.940 \text{ \AA}^3 = 60.08 \text{ \AA}^3$  for STO (001),  $V_{pc} = 3.905^2 \times 3.980 \text{ \AA}^3 = 60.66 \text{ \AA}^3$  for STO (110) and  $V_{pc} = 3.905^2 \times 3.954 \text{ \AA}^3 = 60.29 \text{ \AA}^3$  for STO (111) ( $pc$ : pseudocubic).

The local microstructures of the films were investigated for films grown on (110)- and (111)-oriented STO substrates, and the high resolution TEM results are shown in Fig. 3. For PVO film on (111)-oriented STO substrate, two kinds of domains are observed, marked by I and II in Fig. 3(a). The thickness of the film is estimated to be  $\sim 35 \text{ nm}$ , in agreement with the XRD results. The SAED and high resolution TEM results reveal that the orientation relations for film (F) grown on (111)-oriented STO substrate (S) are: (1)  $F[011]_o // S[111]_c$  and  $F[100]_o // S[110]_c$  (shown in red in Fig. 3(f)), or,  $F[101]_o // S[111]_c$  and  $F[010]_o // S[110]_c$ , the out-of-plane lattice parameters for  $[011]_{PVO}$  and  $[101]_{PVO}$  being almost similar, (2)  $F[311]_o // S[111]_c$  and  $F[\bar{1}\bar{1}2]_o // S[110]_c$  (shown in green in Fig. 3(g)) (the subscript  $c$  indicate cubic notation). These domains are oriented  $60^\circ$  to each other, which is consistent

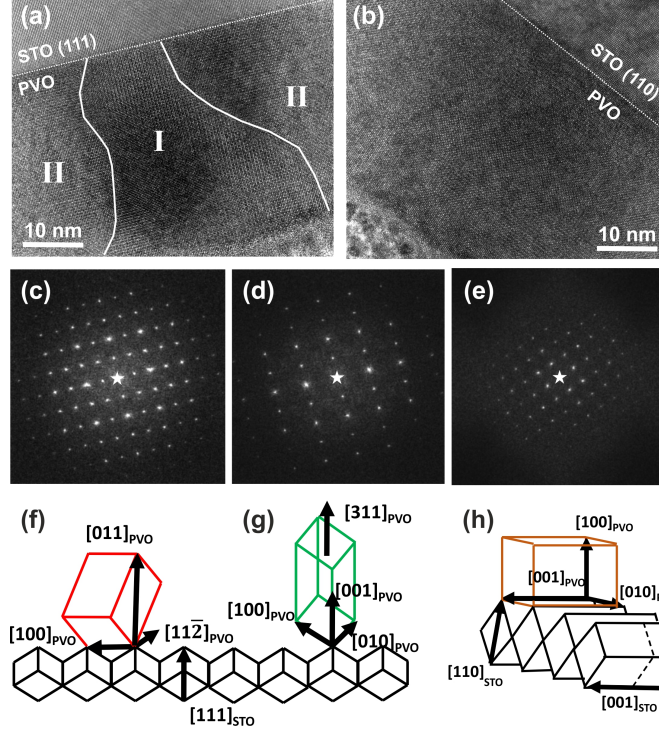


Figure 3: (Color online)(Top panel) HRTEM images of PVO films grown on (a) STO (111) and (b) STO (110) substrates. (Middle panel) (c), (d): Selected area electron diffraction (SAED) patterns for the film on (111)-oriented STO substrate, corresponding to domain I and domain II, respectively. The Zone Axis Point (ZAP) for (c) is along  $[011]_o$  and for (d) is along  $[311]_o$  (the subscript  $o$  refers to orthorhombic). (Middle panel) (e): SAED patterns for the film on (110)-oriented STO substrate, with ZAP along  $[100]_o$ . (Bottom panel) The representative schematics of the observed crystallographic domains in the film on STO (111) (f,g) and STO (110) (h).

with the six fold symmetry presented by the STO (111) substrate. The PVO film on (110)-oriented STO substrate presents a sharp and parallel interface as compared to the interface between film and STO (111) substrate (Fig. 3(b)), in agreement with the previous observations through x-ray diffraction. In addition, the TEM results confirm the thickness of film on STO (110), to be around 35 nm. The diffraction patterns extracted from several different regions in the film indicate presence of only one kind of domain, or, two domains but oriented  $180^\circ$  to each other. Thus, the film grows with  $[100]_o$  (or  $[010]_o$ ) as out-of-plane axis while clamping  $[001]_o$  and  $[010]_o$  (or  $[100]_o$ ) to the substrate, with the following epitaxial relationships:  $F[100]_o$  (or  $F[010]_o$ ) //  $S[110]_c$  and  $F[001]_o$  //  $S[001]_c$ . The observation of different domains on the two substrates is correlated with the crystal symmetries of the substrates. The orthorhombic lattice of (110)-oriented STO (see Fig. 3(h)) may allow coherent growth

of orthorhombic cell of PVO without any atomic reconstruction at the interface, therefore  
 presenting sharp interface in combination with well-defined thickness fringes in the XRD  
 scan. On the contrary, STO(111) substrate is known to undergo atomic reconstruction at  
 the interface to suppress polar discontinuity and its divergent surface energy [18, 19], making  
 this substrate less compatible to grow orthorhombic perovskite lattice. For PVO film grown  
 on (001)-oriented STO substrate, we have already observed two domains, oriented  $90^\circ$  to  
 each other with the epitaxial relationship:  $F[110]_o // S[001]_c$  and  $F[001]_o // S[100]_c / S[010]_c$   
 [2, 9]. In general, the sign and strength of lattice mismatch vary with the orientations of the  
 substrate, and thus different distortions may be induced in the film, yielding different crystal  
 structures. The calculated in-plane lattice mismatches and observed growth orientations of  
 the films for different oriented STO substrates are listed in Table I. The (001)-oriented STO  
 exerts tensile stress on PVO  $[001]_o$ -axis (see Table I), imposing tetragonal distortion on the  
 unit cell [2]. On the other hand, (110)- and (111)-oriented STO substrates would impose

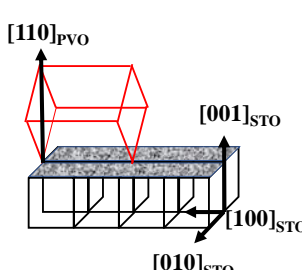
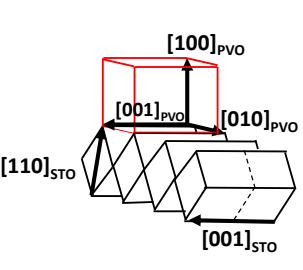
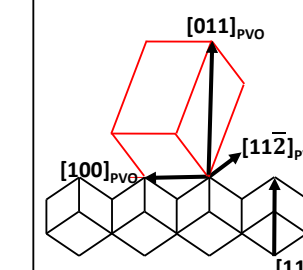
	STO[001]			STO [110]			STO [111]		
	In-plane		Out-of-plane	In-plane		Out-of-plane	In-plane		Out-of-plane
Directions	$[001]_o = [100]_{pc}$	$[\bar{1}\bar{1}0]_o = [010]_{pc}$	$[110]_o = [001]_{pc}$	$[001]_o = [001]_{pc}$	$[010]_o/[100]_o = [110]_{pc}$	$[100]_o/[010]_o = [110]_{pc}$	$[11\bar{2}]_o = [110]_{pc}$	$[100]_o/[010]_o = [110]_{pc}$	$[\bar{1}01]_o/[0\bar{1}1]_o = [111]_{pc}$
Lattice mismatch	0.41 %	-0.05 %		0.41 %	-0.74 % / 0.65 %		0.18 %	0.65 % / -0.74 %	
Growth									

Table I: (Color online) A detailed summary of the in-plane and out-of-plane lattice directions of PVO grown on STO substrates with different orientations. The lattice misfits between in-plane directions of PVO and the substrate are shown. The experimentally observed growth orientations of the PVO lattice on different oriented STO substrates are also shown. Here, a positive lattice mismatch between PVO and substrate indicates tensile stress, and negative indicates compressive stress.



monoclinic and trigonal distortions, respectively, due to unequal lattice mismatches along two in-plane orthogonal directions.

#### IV. MAGNETISM

Since the strain and lattice distortion depend on the orientations of the STO substrates, the magnetic properties of PVO films are expected to differ for the three orientations of the substrate, due to change in the V–O bond length and V–O–V bond angle. The primary magnetic results of 35 nm thick PVO thin films are shown in Fig. 4. For PVO film on the (001)-oriented STO, the saturated magnetization ( $M_s$ ) is  $\sim 0.3 \mu_B$  / f.u., and is close to our earlier observations [2]. Remarkably, the saturated magnetization for PVO films on (110)- and (111)-oriented STO substrates has extensively enhanced, close to  $1.0 \mu_B$  / f.u. and  $2.3 \mu_B$  / f.u., respectively. These obtained values of  $M_s$  are larger as compared to that of the bulk, which is  $\sim 0.6 \mu_B$  / f.u. [8]. Due to the polar nature of the (110)- and (111)-oriented STO substrates, they are more susceptible to the reconstruction. This could allow a quicker recovery of the spin moments, leading to an enhanced magnetization. To the best of our knowledge, this striking phenomenon where the saturated magnetization is increased by approximately 8-fold merely by changing the crystal surface orientation of the substrate, is perhaps observed first time in the oxide thin films. Indeed, a similar study focussed on SrRuO<sub>3</sub> thin films grown on different oriented STO substrates reported nearly 2 times enhancement of saturated magnetization (between (001) and (111)-oriented STO), and the authors explained this peculiar behavior using a high spin state of Ru<sup>4+</sup> ions [20]. However, V<sup>3+</sup> ion has only two electrons in the 3d shell ( $t_{2g}$  orbital-active system), making them ineligible for high spin state context which typically require at least four electrons in the 3d shell. Nevertheless, a dead-layer present at the surface of film and consisting of isolated paramagnetic Pr ions, could also explain the observed substantial magnetization. In fact, we have recently shown that a dead layer of  $\sim 5$  nm in thickness, which is composed of mainly V<sup>4+</sup> ions, is responsible for the increase of magnetization for low thicknesses films [10].

Remarkably, the steps in the hysteresis loops (especially for STO (111)) are also seen, and are almost similar to what were previously reported for PrVO<sub>3</sub> single crystals (below 3 K) [21]. In the stated reference [21], the steps (in hysteresis loop) strongly depended on the field sweep rate, namely, they shifted to a higher magnetic field when sweep rate was decreased. This unusual behavior was then proposed to be arisen on the account of

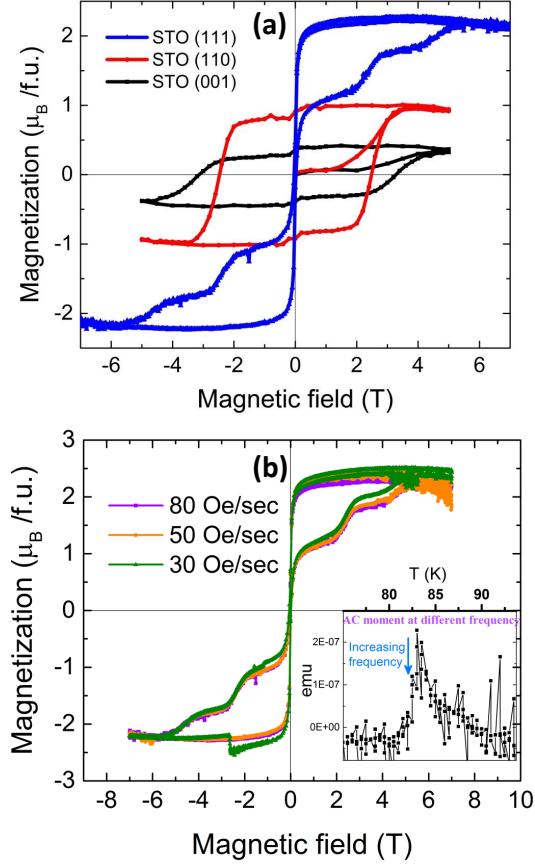


Figure 4: (a) Hysteresis cycles at 10 K for 35 nm thick PVO films on (001)-, (110)- and (111)-oriented STO substrates, obtained by applying magnetic field in the plane of sample. (b) Hysteresis cycles for PVO film on (111)-oriented substrate at different field sweep rates. Inset shows the AC moment of the same sample as a function of temperature (in the vicinity of magnetic ordering temperature) taken at different frequencies.

two phases in  $\text{PrVO}_3$  single crystals, one with the fraction of spins responsible for the glassy-like behavior, and other spins ordered in the antiferromagnetic fashion. Thus, in order to verify if the steps in the hysteresis loops are related to spin-glass-like mechanism, we have collected hysteresis loops for PVO film on (111)-oriented STO at different field sweep rates (Fig. 4(b)), in combination with the AC moment of the sample at different frequencies in the vicinity of magnetic ordering temperature (inset of Fig. 4(b)). We infer that, neither the steps in hysteresis loop depend upon field sweep rate, nor the magnetic ordering temperature show variation as a function of frequency, a necessity for spin glass system. These observations suggest that the steps in the hysteresis loop may not essentially be related to the spin-glass structure, but perhaps to the magnetic domains in the film.

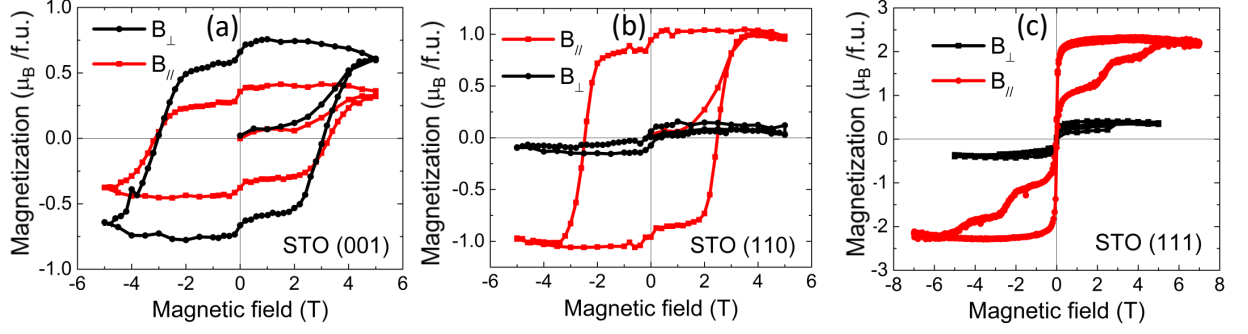


Figure 5: (a)-(c) Hysteresis cycles for films on three oriented STO substrates with field applied along the sample plane and perpendicular to the sample.

The magnetic anisotropy of the PVO films was characterized by  $M$ - $H$  curves after the subtraction of the diamagnetic contribution from the oriented STO substrates. The magnetic field was applied along in-plane and out-of-plane of the sample, and the results are shown in Fig. 5. On one hand, for PVO film on (001)-oriented STO, the largest saturated magnetization within the measured magnetic field range is acquired when magnetic field is applied along out-of-plane direction, and thus regarded as the magnetic easy axis. On the other hand, for films on (110)- and (111)-oriented STO, a strong anisotropy is observed, where, the largest saturated magnetization is achieved for field applied along in-plane of the sample. Therefore, the magnetic easy axis most probably remains normal to the film plane, along PVO  $[110]_o$  for (001)-oriented STO, while it changes along the film plane for (110)- and (111)-oriented STO, along PVO $[001]_o$  and PVO $[11\bar{2}]$ , respectively. This could be due to the deformed  $\text{VO}_6$  octahedra, which is extended (compressed) along out-of-plane direction for a compressive (tensile) strain. A summary of the magnetic parameters; coercive field ( $H_c$ ), remanent magnetization ( $M_R$ ) and saturated magnetization ( $M_s$ ), for field parallel (in-plane) and perpendicular (out-of-plane) configuration, are listed in Table II.

We have further investigated the effect of strain relaxation in PVO films on the uniaxial / biaxial magnetic anisotropy. For this, films of thickness  $\sim 75$  nm were fabricated on the (001)-, (110)- and (111)-oriented STO substrates. The x-ray reciprocal space maps (not shown) recorded for skew symmetrical planes of the substrates show that the films are partially relaxed. Fig. 6 shows the anisotropy results of 75 nm thick films for the three

Table II: Crystallographic orientation and angular dependence of coercive field  $H_c$ , remanent magnetization  $M_R$ , and the saturation magnetization  $M_s$  for 35 nm thick PVO films. Here,  $\theta$  (angle between direction of magnetic field and sample surface) =  $0^\circ$  means field is applied *in-plane*, and  $\theta = 90^\circ$  means field is orthogonal to sample surface.

Orientation		$0^\circ$ / <i>in-plane</i>	$90^\circ$ / <i>out-of-plane</i>
001	$H_c$ (T)	3.1	3.0
	$M_R$ ( $\mu_B$ / f.u.)	0.35	0.66
	$M_s$ ( $\mu_B$ / f.u.)	0.42	0.75
	axis	Hard	Easy
110	$H_c$ (T)	2.4	0.2
	$M_R$ ( $\mu_B$ / f.u.)	0.9	0.06
	$M_s$ ( $\mu_B$ / f.u.)	1.0	0.15
	axis	Easy	Hard
111	$H_c$ (T)	0.03	0.03
	$M_R$ ( $\mu_B$ / f.u.)	0.47	0.03
	$M_s$ ( $\mu_B$ / f.u.)	2.3	0.4
	axis	Easy	Hard

orientations of the substrates. For film on the (001)-oriented STO, the saturated magnetization is largest along the out-of-plane direction of substrate (or film) (Fig. 6(a)), and could be the magnetic easy axis. For two orthogonal in-plane directions of the substrate, we observe similar shapes of the hysteresis loops, along with analogous magnetizations (both saturated and remanence). This indicates isotropic magnetism probably due to dominance of four-fold crystalline anisotropy in the PVO film on (001)-oriented STO substrate.

For (110)-oriented STO substrate, we observe an obvious square-like hysteresis loop with the largest magnetization along in-plane [001] of STO, and perhaps is the magnetic easy axis. While the hard axis lies along out-of-plane [110] of the STO, as evidenced by the linear hysteresis loop (inset of Fig. 5(b)). Therefore, PVO film on the (110)-oriented STO substrate noticeably shows a perpendicular anisotropy. Interestingly, the magnetization along the two in-plane orthogonal directions differ extensively. This clearly shows the presence of uniaxial anisotropy for film on (110)-oriented STO substrate, and can be account for the magnetoelastic anisotropy present in the film due to unequal lattice mismatch along two in-plane directions. Finally, for the PVO film on (111)-oriented STO, the magnetic easy axis is along

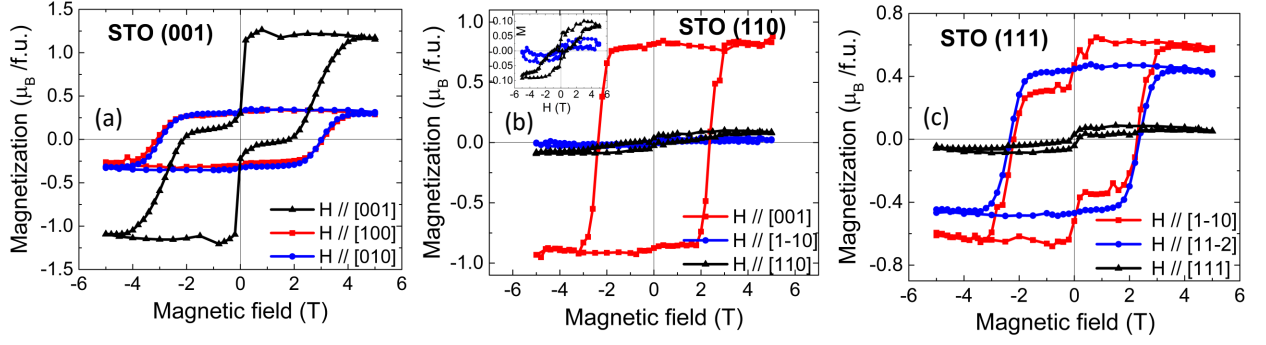


Figure 6: The hysteresis loops of 75 nm thick PVO films on (a) (001)-, (b) (110)- and (c) (111)-oriented STO substrates, along two in-plane and out-of-plane directions of the substrates.

any of the in-plane directions, and the hard axis remains along the out-of-plane  $[111]$ -axis direction of the substrate. The remanences of the two in-plane directions are nearly equal, although the saturated magnetization remains higher along  $[1\bar{1}0]$  direction. Also, given the six-fold symmetry of the STO (111), the easy axis could lie along any of the in-plane axis besides  $[1\bar{1}0]$  and  $[11\bar{2}]$  which stabilizes the energy balance between magnetocrystalline energy and both magnetostatic and magnetostriction energy. The deformation of the oxygen octahedra surrounding V, elongated and compressed along the out-of-plane direction for compressive and tensile strain, respectively, can be at the origin of the observed magnetic anisotropy. Moreover, in the present case, the in-plane strains are unequal along the two in-plane orthogonal directions, producing further in-plane deformation of the octahedra, and thus causing in-plane uniaxial anisotropy. However, the direction of the magnetic easy axis along out-of-plane (probably) for STO (001), and along in-plane for STO (110) and STO (111), is still confusing. In general, the compressive strain enhances the out-of-plane magnetization, while tensile strain increases the in-plane magnetization [14, 22, 23]. Accordingly, we have estimated an approximate pseudocube expansion (compare with bulk) of the unit cell of PVO for the three orientations of the substrate, to be  $\sim 1.2\%$  (STO (001)),  $\sim 2.5\%$  (STO (110)) and  $\sim 1.7\%$  (STO (111)). From our earlier report [2], we know that the tensile strain in PVO expands the unit cell, whereas, the compressive strain effectively reduces the unit cell volume of PVO. Therefore, in this sense, STO (110) and STO (111) substrates probably impose more tensile strain on the unit cell of PVO, forcing the magnetic easy axis to stay along in-plane direction. On the other hand, film on STO (001) can favor a weak out-of-plane anisotropy (present case), or no anisotropy at all (in Ref. [1]) due to a negligible tensile strain.

## V. CONCLUSIONS

In summary, we have studied the magnetic anisotropy of  $\text{PrVO}_3$  thin films on the oriented  $\text{SrTiO}_3$  substrates. We have found that the magnetization of  $\text{PrVO}_3$  thin film on (111)-oriented  $\text{SrTiO}_3$  substrate can be extensively enhanced compare to the bulk. All the films clearly show magnetic anisotropy. While films on the (001)-oriented  $\text{SrTiO}_3$  show a weak out-of-plane anisotropy, a strong in-plane anisotropy is observed for films grown on the (110)- and (111)-oriented  $\text{SrTiO}_3$  substrates. Furthermore, an evident uniaxial anisotropy is also argued for films on the (110)-oriented  $\text{SrTiO}_3$  substrates, and would probably require further experiments, e.g., XPS/XAS, X-ray Magnetic Circular Dichroism (XMCD) in order to confirm a dead layer on the surface of the films (especially for film on  $\text{STO}(111)$ ) and to observe the magnetism from individual cations, respectively.

## Acknowledgments

DK thanks Maxime Hallot for preparing cross section of the samples and F. Veillon for his valuable experimental support. The authors also thank to S. Froissart for the AFM support and L. Gouleuf for technical support. DK thanks O Copie and U Lüders for illuminating discussions. This work is supported by Region Normandie, by french ANR POLYNASH (ANR-17-CE08-0012) and Labex EMC3.

- 
- [1] O. Copie, J. Varignon, H. Rotella, G. Steciuk, P. Boullay, A. Pautrat, A. David, B. Mercey, P. Ghosez, and W. Prellier, *Adv. Mater.* **29**, 1604112 (2017).
  - [2] D. Kumar, A. David, A. Fouchet, A. Pautrat, J. Varignon, C.U. Jung, U. Lüders, B. Domengès, O. Copie, P. Ghosez, and W. Prellier, *Physical Review B* **99**, 224405 (2019).
  - [3] J.A. Moyer, C. Eaton, and R. Engel-Herbert, *Adv. Mater.* **25**, 3578 (2013).
  - [4] H.-T. Zhang, M. Brahlek, X. Ji, S. Lei, J. Lapano, J.W. Freeland, V. Gopalan, and R. Engel-Herbert, *ACS Appl. Mater. Interfaces* **9**, 12556 (2017).
  - [5] C. Wang, H. Zhang, K. Deepak, C. Chen, A. Fouchet, J. Duan, D. Hilliard, U. Kentsch, D. Chen, M. Zeng, X. Gao, Y.-J. Zeng, M. Helm, W. Prellier, and S. Zhou, *Phys. Rev. Materials* **3**, 115001 (2019).
  - [6] S. Miyasaka, Y. Okimoto, M. Iwama, and Y. Tokura, *Phys. Rev. B* **68**, 100406(R) (2003).

- [7] M.H. Sage, G.R. Blake, C. Marquina, and T.T.M. Palstra, Physical Review B 76, 195102 (2007).
- [8] F. Wang, J. Zhang, P. Yuan, Q. Yan, and P. Zhang, Journal of Physics: Condensed Matter 12, 3037 (2000).
- [9] O. Copie, H. Rotella, P. Boullay, M. Morales, A. Pautrat, P.-E. Janolin, I.C. Infante, D. Pravathana, U. Lüders, and W. Prellier, Journal of Physics: Condensed Matter 25, 492201 (2013).
- [10] D. Kumar, A. Fouchet, A. David, A. Cheikh, T.S. Suraj, O. Copie, C.U. Jung, A. Pautrat, M.S. Ramachandra Rao, and W. Prellier, Phys. Rev. Materials 3, 124413 (2019).
- [11] Y. Hotta, H. Wadati, A. Fujimori, T. Susaki, and H.Y. Hwang, Applied Physics Letters 89, 251916 (2006).
- [12] A. Fouchet, J.E. Rault, M. Allain, B. Bérini, J.-P. Rueff, Y. Dumont, and N. Keller, Journal of Applied Physics 123, 055302 (2018).
- [13] P. Zhou, Y. Qi, C. Yang, Z. Mei, A. Ye, K. Liang, Z. Ma, Z. Xia, and T. Zhang, AIP Advances 6, 125044 (2016).
- [14] H. Boschker, M. Mathews, E.P. Houwman, H. Nishikawa, A. Vailionis, G. Koster, G. Rijnders, and D.H.A. Blank, Phys. Rev. B 79, 214425 (2009).
- [15] L. You, C. Lu, P. Yang, G. Han, T. Wu, U. Luders, W. Prellier, K. Yao, L. Chen, and J. Wang, Adv. Mater. 22, 4964 (2010).
- [16] D. Kan, R. Aso, R. Sato, M. Haruta, H. Kurata, and Y. Shimakawa, Nature Mater 15, 432 (2016).
- [17] C.U. Jung, H. Yamada, M. Kawasaki, and Y. Tokura, Appl. Phys. Lett. 84, 2590 (2004).
- [18] J.L. Blok, X. Wan, G. Koster, D.H.A. Blank, and G. Rijnders, Applied Physics Letters 99, 151917 (2011).
- [19] J. Chang, Y.-S. Park, and S.-K. Kim, Appl. Phys. Lett. 92, 152910 (2008).
- [20] A. Grutter, F. Wong, E. Arenholz, M. Liberati, A. Vailionis, and Y. Suzuki, Applied Physics Letters 96, 082509 (2010).
- [21] L.D. Tung, Physical Review B 72, 054414 (2005).
- [22] F. Tsui, M.C. Smoak, T.K. Nath, and C.B. Eom, Appl. Phys. Lett. 76, 2421 (2000).
- [23] J. Dho, Y.N. Kim, Y.S. Hwang, J.C. Kim, and N.H. Hur, Appl. Phys. Lett. 82, 1434 (2003).